FLOWER

Flax composites, LOW weight, End of life and Recycling

research • cooperation • performance • flax • biocomposites • recycling • automobile • sailing • advertising • fibre • lightweighting •

EUROPEAN UNION

Deliverable n°T.3.5.1

Technical report of the numerical modelling of flax fibres and rovings

03/2023

TVDC

Université Bretagne Sud ubs : INRAE UNIVERSITY OF PORTSMOUTH UNIVERSITY OF CAMBRIDGE

Depestele Teillage Vandecandelaere kairos environnement EcoTechnilin HOWA TRAMICO

Interreg France (Channel Manche) England

EUROPEAN UNION

European Regional Development Fund

Partners

PP Leader : TVDC

Partners involved : Kairos, HOWa-TRAMICO, UCam, UPort

Content

Context

During the extension of the FLOWER project, a collaboration between DEPESTELE and the LAMé laboratory in Orléans led to work on modeling the deformation of the dry reinforcements, in order to be able to take into account, during the design, the place that the fibers will occupy after compaction, either by manual action for the "hand lay-up" with or without compaction, or by vacuum in the case of infusion processes, or by a press in the case of implementation by RTM technology.

These elements are not taken into account during the modeling of finished composite parts by considering the layers of reinforcements as homogeneous and whose properties are established by mechanical tests and homogenized during the calculation by finite elements.

By experience, the person skilled in the art knows the deformation that the pressure field applied to the dry reinforcement, before the introduction of the resin, will induce and arranges the reinforcement elements “at best” without a theoretical basis.

More precisely, the fibrous elements within a reinforcement will also be likely to move and adopt conformations linked to the available space and/or to the deformation/crushing of the fibers themselves.

This report aims to present the advances in the simulation at the mesoscopic scale of the shaping of a dry reinforcement based on flax rovings with a hypo-elastic model (VUMAT Hypo) at first, and hyper-elastic (VUMAT Hyper) in a second step.

Integration of the Hypoelastic VUMAT under ABAQUS

As part of the so-called LCM (Liquid Composite Molding) processes, mastering the first step of forming dry reinforcements plays an essential role in the integrity of the reinforcement and the positioning of the fibers.

Figure 1 : Etapes de fabrication d'un composite par procédé LCM

Poor preforming management will therefore influence the behavior of the final composite part. It is therefore important to characterize this step by studying the behavior of the reinforcements. Although it is possible to directly carry out tests allowing to know the mechanical behavior and the mechanisms of deformations and damages, this remains complex and expensive to implement. The advantage of setting up a simulation would make it possible to predict the feasibility of the parts in advance and to optimize the processes.

The reinforcement has three level of studies :

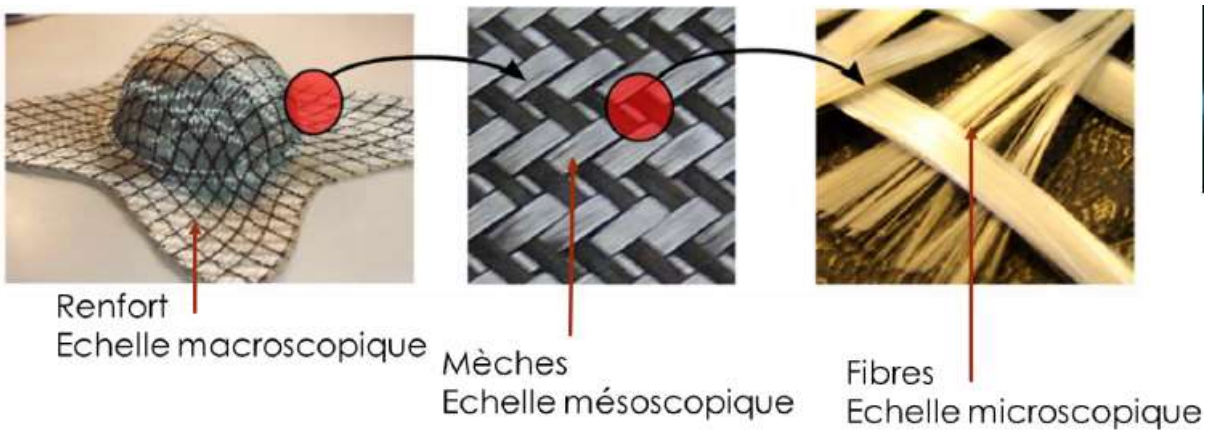

Figure 2 : Les différentes échelles du renfort

Each scale has its advantages and disadvantages:

- At the macroscopic scale, the fabric is modeled by a membrane and does not explicitly include the interlacing of the rovings, which does not make it possible to obtain precisely the mechanical behavior of the fabric.
- On the other hand, the microscopic scale takes into account the distribution and the contact of thousands of fibers which is, today, too complex and very costly in terms of calculation time.
- The mesoscopic scale, for its part, includes the intertwining of supposedly homogeneous rovings and therefore makes it possible to obtain results that are both global (reinforcement in the deformed state for example) but also local

(deformation of the rovings, variation in the shape of the sections, etc.). This scale therefore seems to be, today, the best compromise between precision of the behavior and complexity of the simulation.

In order to set up the simulation of the reinforcement, it is therefore necessary to study the rovings which compose it and to obtain, through tests and numerical simulations, a law of behavior and a coherent geometry. For this study, the rovings are flax rovings, i.e. an assembly in the form of a ribbon of long, discontinuous aligned fibers held together by a binder.

Methodology and strategy

The strategy applied in obtaining the reinforcement simulation during the thesis is as follows:

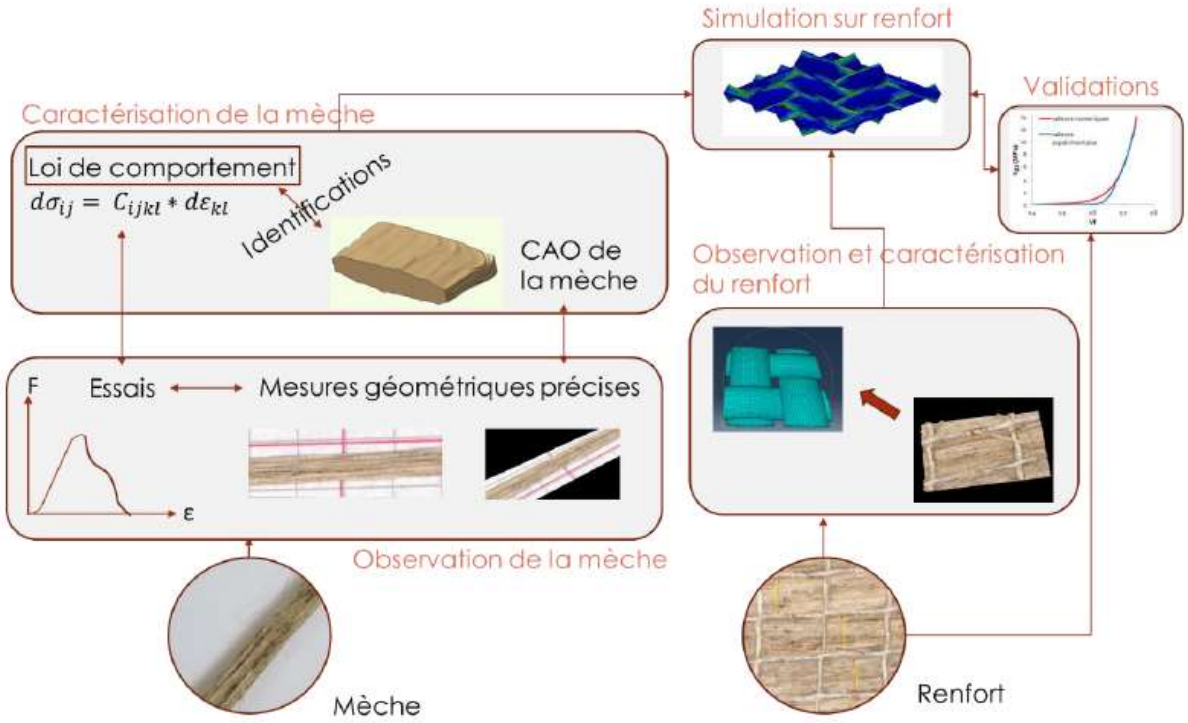

Figure 3 : Stratégie de modélisation

First, the strategy consists in studying the roving in order to extract from it a hypoelastic constitutive law of an equivalent homogeneous transverse isotropic material.

A study of the geometry of the rovings before weaving was carried out. This study made it possible to observe the strong geometric disparity of linen rovings but made it possible to identify the shape of the sections as well as a statistical distribution of the different geometric sizes. This highlighted the importance of taking these variations into account in the model.

Experimental and numerical tests have been set up on the roving in order to obtain the equivalent homogeneous behavior law. Then observations and characterization of the reinforcement are carried out before carrying out a simulation of the reinforcement and a validation phase of this simulation.

Concerning the hypotheses on the constitutive law, the choice was made to work with an existing hypoelastic constitutive law already applied to synthetic fibers such as:

$$d\sigma_{ij} = C_{ijkl} * d\varepsilon_{kl}$$

Avec

$$[C_{fi}] = \begin{bmatrix} C_{1111} & 0 & 0 & 0 & 0 & 0 \\ \cdots & C_{2222} & C_{2233} & 0 & 0 & 0 \\ \cdots & \cdots & C_{3333} & 0 & 0 & 0 \\ \cdots & \cdots & \cdots & C_{1212} & 0 & 0 \\ \cdots & \cdots & \cdots & \cdots & C_{2323} & 0 \\ \cdots & \cdots & \cdots & \cdots & \cdots & C_{1313} \end{bmatrix}$$

the transverse isotropic behavior tensor connecting the stress increment of Cauchy to the strain increment in the base fi.

The different coefficients of this tensor can be identified from elementary tests such as:

$$C_{1111} = \frac{K}{S_m} \rightarrow \text{identifiable avec un essai de traction}$$

- K : rigidité en traction (N)
- S_m : section de la mèche (mm^2)

The variable being constant in this law, the first simulation results will therefore be with a mean section representative of the roving. However an adaptation of this law allowing the taking into account of the variability of the sections is envisaged.

$$C_{2222} = C_{3333} = \frac{K_c * \gamma * V_f^{\gamma}}{1 + \nu_{23mat} * V_f^{n-1}}$$

$$C_{2233} = \frac{K_c * \gamma * \nu_{23mat} * V_f^{n-1+\gamma}}{1 + \nu_{23mat} * V_f^{n-1}}$$

$$C_{2323} = \frac{(1 - \nu_{23mat} * V_f^{n-1}) K_c * \gamma * V_f^{\gamma}}{1 + \nu_{23mat} * V_f^{n-1}}$$

➔ Identifiable with a compaction trial

- K_c, γ : Paramètre de Toll obtenue en exprimant la pression exercée sur le roving en fonction de la fraction volumique de fibres.
- V_f : fraction volumique de fibres au sein de la mèche
- ν_{23mat} : coefficient de Poisson du lin
- n : à identifier sur la courbe des déformations

$$C_{1212} = C_{1313} \rightarrow identifiables\ avec\ un\ essai\ de\ flexion\ de\ type\ Peirce$$

Experimental trials

Tensile test

In order to obtain the parameter K of the coefficient C111 behavior law, a tensile test must be carried out on the roving. The test consists of extracting the deformation within the roving by tracking markers. This method allows us in particular to overcome the rigidity of the traction device (often called compliance). Moreover, having an assembly of discontinuous fibers, the deformation of the roving is not homogeneous in the length. Finally, there is a very strong disparity in the results observed and this will require a statistical study with numerous tests.

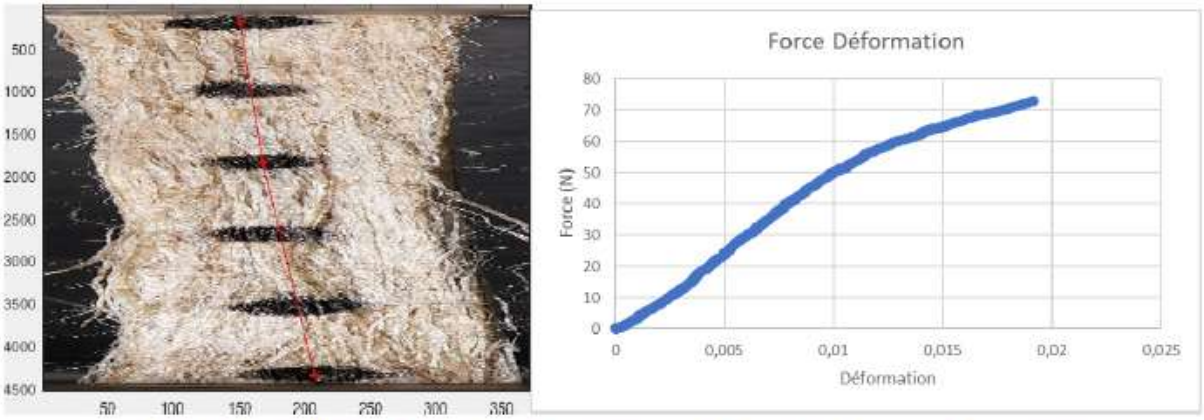

Figure 4 : Exemple de courbe obtenue par suivi de marqueurs lors d'un essai de traction

The reorientation of the fibers within the bundles and of the bundles within the wick results in the curve obtained being divided into three zones, the stiffness K of the wick being obtained in the linear part (2):

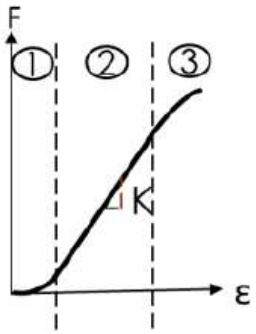

Figure 5 : Courbe de traction pour une mèche de lin

This non-linear part at the start of the curve leads to overestimating the force necessary with the current constitutive law in the numerical modeling by directly using K. It will therefore be necessary in a second step, once the model has been developed, to take into account in the constitutive law the non-linearity of behavior in traction.

To preserve linearity in the short term, two approximations are possible:

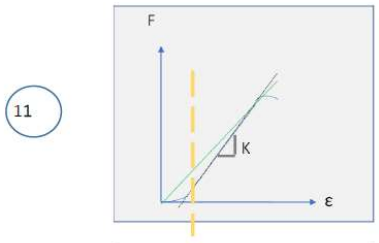

Une approximation complètement linéaire de la courbe dont on utilise la pente (K') à la place de K

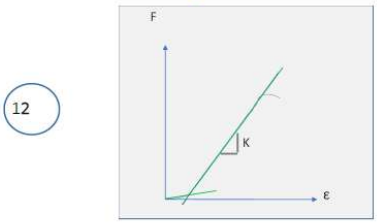

Une approximation de la courbe avec deux droites, la deuxième reprenant K

The first case is applicable if the deformation in the first nonlinear zone is weak. On the other hand, if this is not the case then the second case is the most adequate model but requires modifying the form of the constitutive law implemented in the simulations, also called Vumat. The statistical study that must be carried out will make it possible to conclude on the need or not to engage in case 2.

The tensile tests already carried out have also confirmed that the average tensile stiffness depends on the gauge length. At this time, it is not possible to take this aspect into account in the behavior model, especially since the impact of this point on the behavior of the reinforcement is not established. This point will have to be considered in the second level of modelling. This will require performing several numerical tests at different gauge lengths in order to validate our approach.

Compaction / compression test

Concerning the compaction/compression test, this will be studied through two tests in order to observe on the one hand the reorganization of the fibers during the compaction phase (only the variations of the fiber envelope between stages 1 and 2 of Figure 6) and on the other hand the compression.

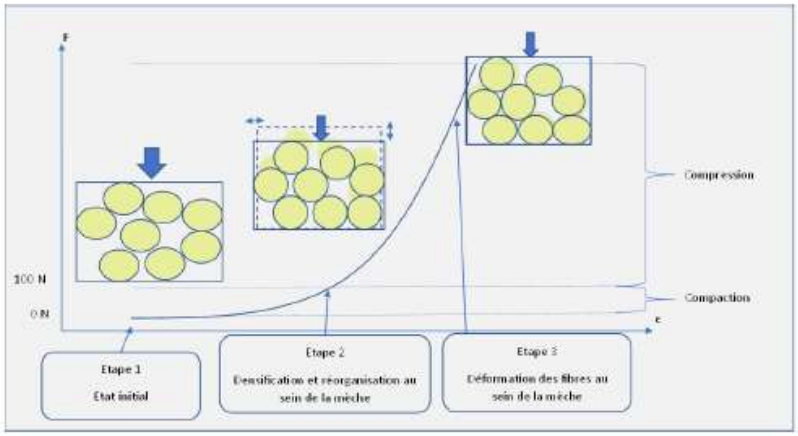

Figure 6 : Courbe théorique d'un essai de compression du roving

Indeed, it was found that it was possible to observe the compaction of the roving under load from the microscope:

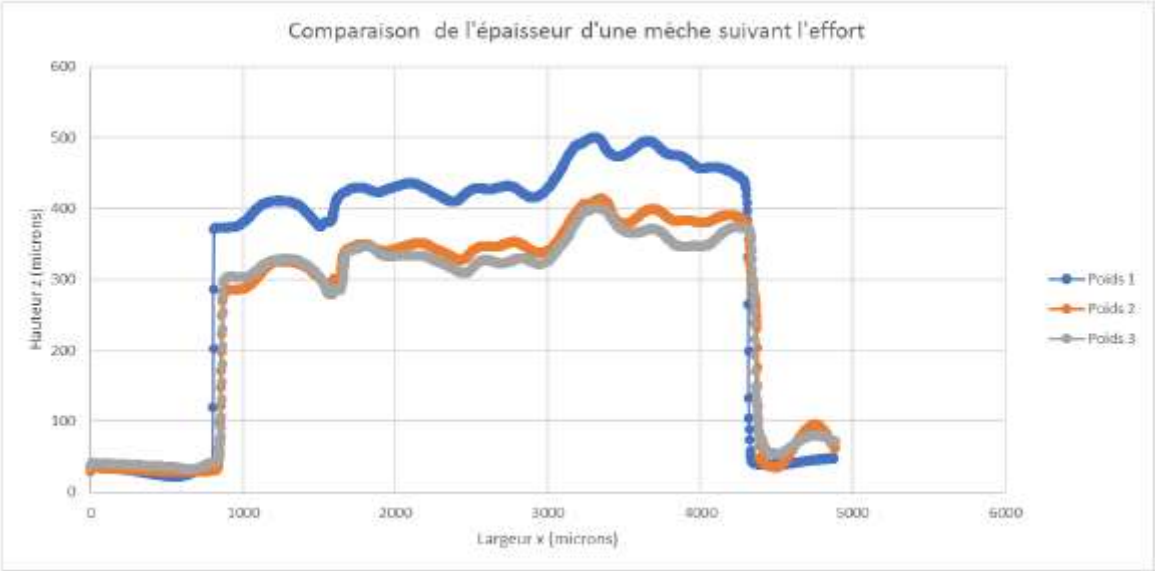

Figure 7 : Evolution d'une section d'un roving sous différentes charges

Thanks to the 3D reconstruction of the initial state of the roving and of each stage under load, it is possible to finely compare the digital simulation of the compaction test and the experimental test. In order to correctly manage the distribution of the force on the roving during the test, a device has been developed.

The compression part of the roving is studied with the traction machine. The settings Kc, Y Toll's y are identified from the curve obtained as a function of the evolution of the pressure and of the fiber volume fraction. In order to follow the evolution of the sections being compressed, a pressure sensor (piezoelectric) will be installed.

Digital models

The initial constitutive law takes into account only a modeling with a constant section. The roving is therefore modeled by a rectangular parallelepiped (in agreement with the observations on the shape obtained by measurements on a digital microscope).

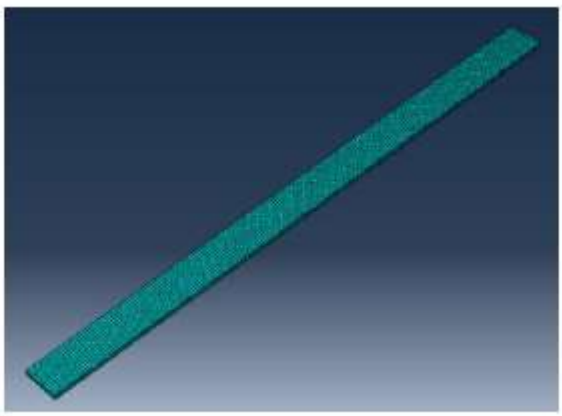

Figure 8 : Modèle numérique d'un roving à section constante (Modèle 1)

We have underlined the importance of taking into account the variability of the sections along the specimen. A digital model obtained from the scan of a specimen via a digital microscope was tested.

Microscope Modèle Catia Modèle Abaqus

Figure 9 : Obtention d'un modèle numérique de roving utilisable pour la simulation numérique à partir d'une image 3D provenant du microscope numérique

The mesh being complex, the model has been simplified. The measurements used to estimate the characteristics of the sections are reused in order to obtain a model in which each section is a rectangle.

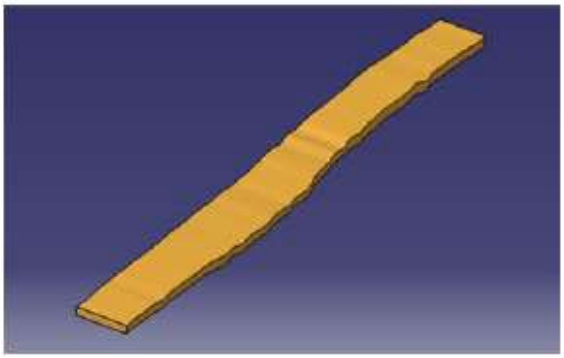

Figure 10 : Modèle numérique d'un roving à sections rectangulaires non constantes (Modèle 2)

This makes it possible to optimize the loading time of the points in CatiaV5, to simplify the volume reconstruction and to obtain a mesh more simply while preserving the variability of the sections of the "scanned" rovings.

Although this section variation does not change the tensile results (physically there is always the same number of fibers in tension according to our assumptions), this consideration is very important in the compaction / compression of the roving. The Vumat and therefore the constitutive law have been modified to take into account the variation in section. Elementary experimental and numerical tests will make it possible to validate the models and the changes in constitutive law.

Numerical simulation

The simulations are performed explicitly such that at any time:

$$[M]\{\ddot{u}\} + [C]\{\dot{u}\} + \{F_{int}\} - \{F_{ext}\} = 0$$

With Fint and Fext the internal and external forces respectively, [M] the diagonalized mass matrix and [C] the damping matrix. In addition: where [K] is the stiffness matrix and α, β are damping coefficients

Tensile test

The initial Vumat takes into account the previously defined parameters with the addition of the longitudinal shear modulus. In the case of a pure tensile test, only the parameters K, and are to be defined. The other parameters are left at the values used during the previous study on synthetic fibers and will be defined later. A first simulation was carried out with model 1 and compared to a test on a 50mm long specimen.

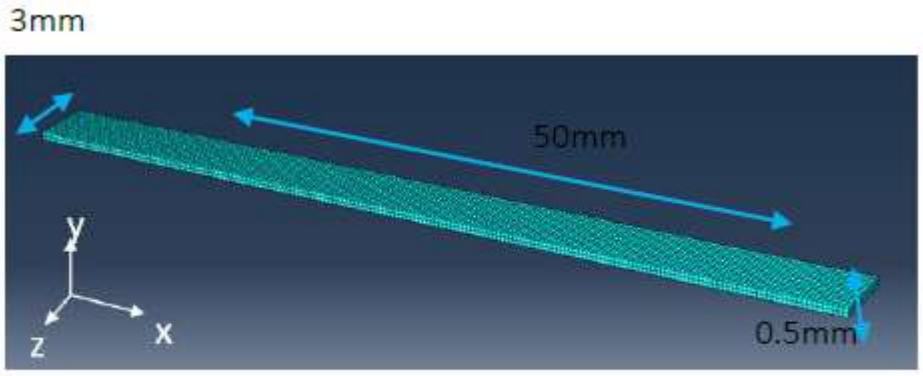

Figure 11 : Modélisation du roving dans Abaqus

En utilisant la loi de comportement hypoélastique et le résultat de l'approximation linéaire de l'essai de traction (K=5310 et K'=4957) nous devions obtenir pour une déformation de 1% avec K', $S_m = 1.5mm^2$ et $\nu = 0.2$:

$\sigma_{11} = \frac{K'}{S_m} = 35.40MPa$ et $F_{11} = 53.10N$.

La simulation (Figure 12) donne à 1% de déformation :

$\sigma_{11} = 35.54MPa$ et $F_{11} = 53.31N$

soit un écart relatif de 0.39% ce qui valide la simulation.

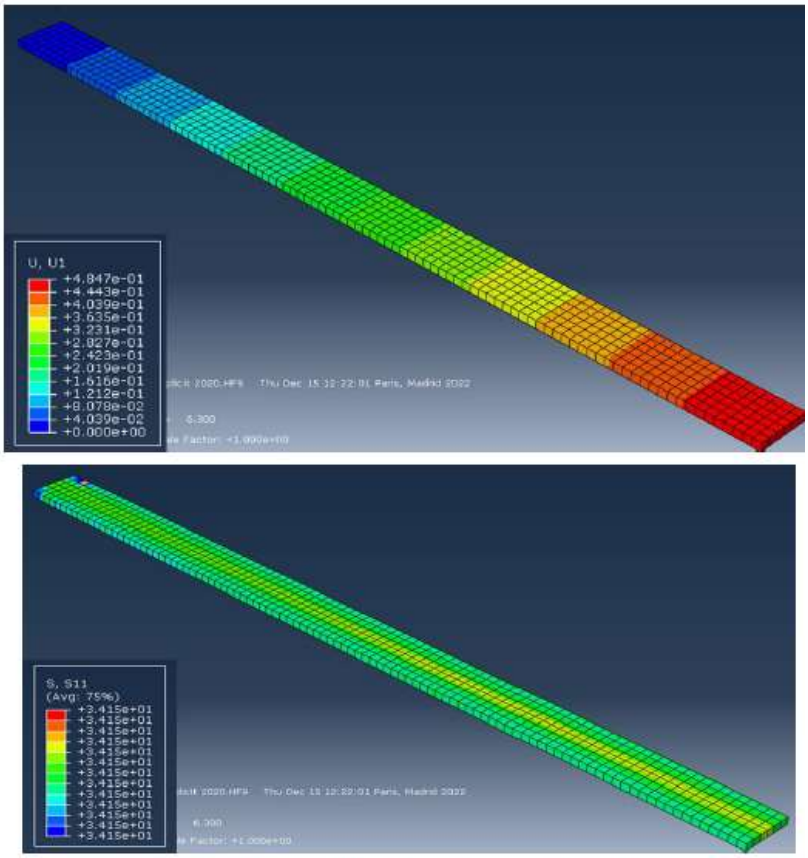

Figure 12 : Résultat de la simulation numérique

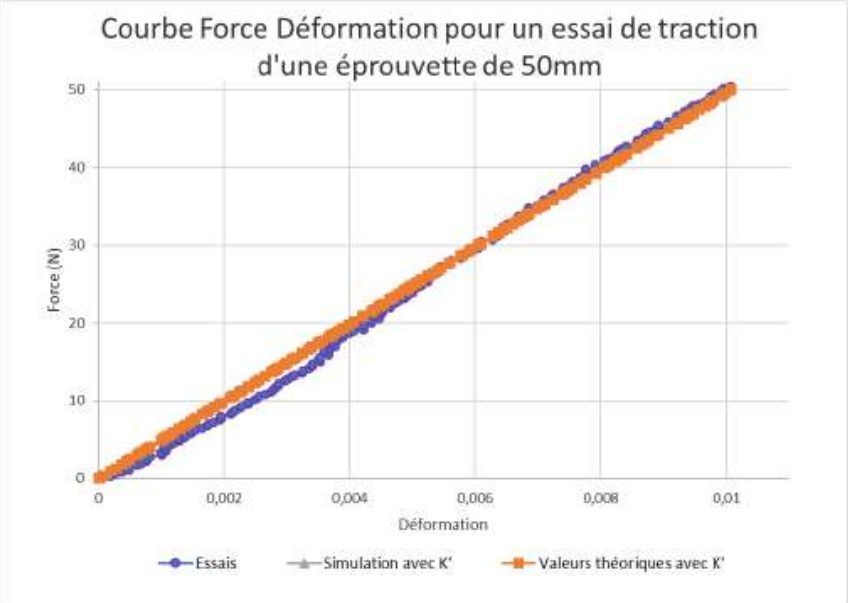

Figure 13 : Comparaison des résultats théoriques et de simulation avec la courbe expérimentale

Before testing the modeling of case 2, we propose here to manually find 2 straight lines modeling the experimental curve. Moreover, one plots the curves of the relative differences between the modelizations and the experimental curve.

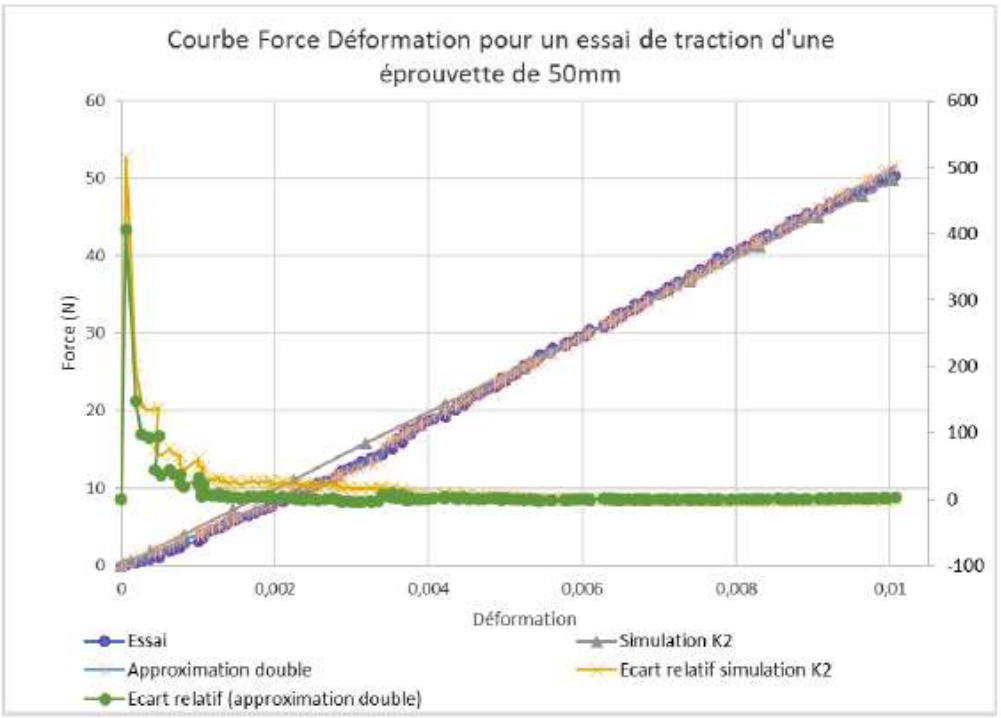

Figure 14 : Comparaison de la courbe d'un essai de traction avec les deux possibilités de modélisation linéaire

It is noticed that the profit on the reduction of the relative error for the nonlinear part is rather weak even with this modeling. If case 2 does not occur very often during the test campaign, it will not be considered for the moment in the numerical modelling.

The test with K' is repeated with model 2 and the two formulations of the constitutive law (C1111 with or constant section).

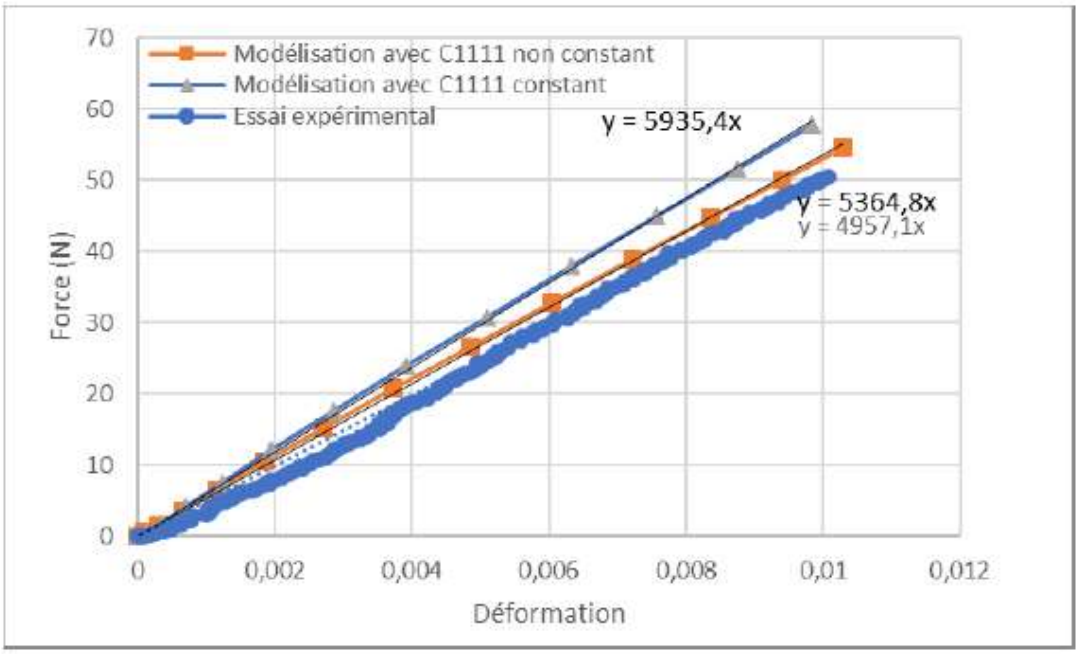

Figure 15 : Comparaison de la courbe d'un essai de traction expérimentale avec le modèle 2 et les 2 formulations de la loi de comportement

It is noticed with this model that the use of the law of behavior (VUMAT) taking into account nonconstant sections gives better results. However, a difference of 6% is observed with the desired value. This comes from the increase in the coefficient of the shear modulus which made it possible to stabilize the simulation. Indeed, the scanned model is slightly curved. This implies that the test performed digitally is not quite a pure tensile test but takes bending into account. The increase in this modulus therefore artificially stiffens the wick. The realization of a test with an uncurved model will be studied to validate this hypothesis. However, if the increase in modulus does not influence the other tests, a readjustment of the initial stiffness value could be considered.

Integration of the hyperelastic VUMAT under ANSYS

We have developed a hypoelastic model operating under ABAQUS and The natural continuation of this study is to be able to implement, in the ANSYS computer code, the material behavior law of a flax wick whose mechanical behavior is particular. This specific law does not currently exist in the ANSYS code, it must be developed to allow the study of the mechanical behavior of assemblies of woven flax rovings. The study is carried out with the USERMAT and MAPDL applications of the ANSYS software in version 2021 R2.

The flax roving has a hyperelastic physical behavior, whose material law is close to that defined by A. CHARMETANT in his thesis entitled "Hyperelastic approaches for modeling

the mechanical behavior of woven composite preforms", and dated 2011. The goal is therefore to take this material law, to code it, to implement it in the ANSYS code and to use it for finite element calculations on flax fibres.

Méthodes d'implémentation d'une loi matériau (VUMAT) avec ANSYS

Le logiciel ANSYS dispose d'un outil performant, appelé USERMAT, permettant à l'utilisateur de programmer une loi de matériau spécifique de son choix, et de l'intégrer dans le calcul éléments finis qu'il souhaite réaliser à l'aide de l'application MAPDL.

USERMAT n'est compatible qu'avec MAPDL, il inclue 18 familles d'éléments (LINK180, SHELL181, PLANE182, PLANE183, SOLID185, SOLID186, SOLID187, BEAM188 et BEAM189).

La routine codée via USERMAT sera appelée à tous les points d'intégration de ces éléments durant la phase de résolution du calcul. Le paramètre d'entrée faisant appel à la routine USERMAT dans MAPDL est la commande : TB, USER. La routine USERMAT est donc utilisée pour définir la relation contrainte/déformation ou raideur du matériau. Donc, son comportement mécanique. Pour chaque itération de Newton Raphson, USERMAT est appelé à chaque point d'intégration du matériau. Ansys calcule la contrainte et la déformation à chaque début de l'incrément de temps et de l'incrément de déformation en cours. USERMAT doit également fournir la matrice jacobienne du matériau qui représente sa raideur et qui est égale à $\partial \sigma / \partial \xi$.

Les tenseurs de contrainte, déformation et le Jacobien du matériau sont stockés sous forme vectorielle et matricielle d'ordre différents.

Loi de comportement matériau de la mèche sèche de lin

Dans cette étude, nous avons considéré que la mèche de lin a un comportement mécanique hyperélastique, proche de celle décrite par A. CHARMETANT.

À partir de là, plusieurs hypothèses sont émises pour reproduire sa loi matériau : Une mèche est un assemblage de fibres orientées approximativement dans la même direction. Cet assemblage est supposé suffisamment compact pour que les fibres ne puissent pas se déplacer de façon indépendante. Cette hypothèse permet de considérer ce matériau « mèche » comme un matériau continu.

Ce matériau homogénéisé présente alors une direction privilégiée qui est celle des fibres qui la constituent. La distribution des fibres dans une section de la mèche déformée, est supposée isotrope. La mèche de lin sera donc supposée isotrope transverse.

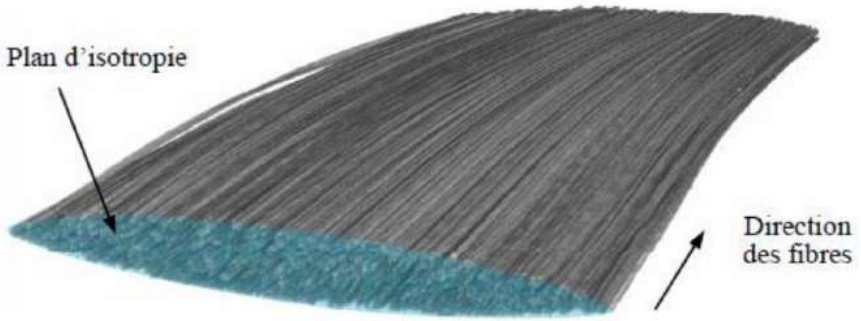

Figure 16 - Représentation d'une section de mèche de lin

The wick behavior law is governed by 4 main deformation modes:
1. Elongation in the direction of the fibers
2. Compaction in the transverse plane
3. Distortion in the transverse plane
4. Shear
5. Transverse

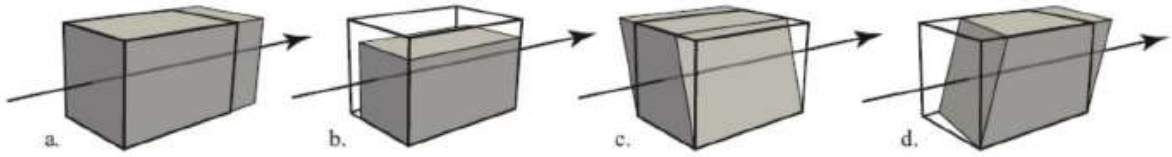

. Modes de déformation de la mèche (la flèche désigne la direction des fibres) :
(a) élongation (b) compaction (c) distorsion (d) cisaillement transverse

To determine the constitutive law of the material, the gradient of the transformation (F) is broken down according to the 4 modes of deformation defined in the preceding paragraph. From this gradient (F), the right Cauchy Green strain tensor (C) is calculated

$$C = F^T.F$$

And leads on the classical invariants:

$$\bar{I}_1 = \mathrm{tr}\bar{\underline{\underline{C}}},$$
$$\bar{I}_2 = \tfrac{1}{2}(\mathrm{tr}^2\bar{\underline{\underline{C}}} - \mathrm{tr}\bar{\underline{\underline{C}}}^2),$$
$$\bar{I}_4 = \underline{a}\cdot\bar{\underline{\underline{C}}}\cdot\underline{a},$$
$$\bar{I}_5 = \underline{a}\cdot\bar{\underline{\underline{C}}}^2\cdot\underline{a}, \qquad I_3 = \det\underline{\underline{C}} \qquad J = \sqrt{I_3}$$

These invariants bearing physical meaning are determined from classical invariants resulting from the right Cauchy Green deformation tensor. Each of these so-called "physical" invariants and depending on the classical invariants usually defined for a hyperelastic material:

Elongation	$I_{along} = \frac{1}{2}\ln(I_4)$
Compaction	$I_{comp} = \frac{1}{4}\ln\left(\frac{I_3}{I_4}\right)$
Distorsion	$I_{dist} = \frac{1}{2}\ln\left(\frac{I_1 I_4 - I_5}{2\sqrt{I_3 I_4}} + \sqrt{\left(\frac{I_1 I_4 - I_5}{2\sqrt{I_3 I_4}}\right)^2 - 1}\right)$
Cisaillement transverse	$I_{cis} = \sqrt{\frac{I_5}{I_4^2} - 1}$

From these physical invariants follows the determination of the strain energy potential:

$$w_{along}\left(I_{along}\right) = \begin{cases} W_{along}^{nl}\left(I_{along}\right) & \text{si } I_{along} \le I_{along}^{0} \\ W_{along}^{lin}\left(I_{along}\right) & \text{si } I_{along} > I_{along}^{0} \end{cases}$$

$$w_{comp}\left(I_{comp}\right) = \begin{cases} K_{comp}\left|I_{comp}\right|^{p} & \text{si } I_{comp} \le 0 \\ 0 & \text{si } I_{comp} > 0 \end{cases}$$

$$w_{dist}\left(I_{dist}\right) = \frac{1}{2}K_{dist}{I_{dist}}^{2}$$

$$w_{cis}\left(I_{cis}\right) = \frac{1}{2}K_{cis}{I_{cis}}^{2}$$

La contrainte de Piola-Kirchoff est déterminée comme étant $\underline{\underline{S}} = 2\frac{\partial W}{\partial \underline{\underline{C}}}$

$$\underline{\underline{S}}_{along} = \frac{1}{I_4}\underline{\underline{M}} \begin{cases} \dfrac{K^0_{along}}{S_0} I_{along} + \dfrac{K_{along} - K^0_{along}}{2S_0 I^0_{along}} I^2_{along} & \text{si } I_{along} \le I^0_{along} \\ -\dfrac{K_{along} - K^0_{along}}{2S_0} I^0_{along} + \dfrac{K_{along}}{S_0} I_{along} & \text{si } I_{along} > I^0_{along} \end{cases}$$

$$\underline{\underline{S}}_{comp}\left(I_{comp} \le 0\right) = -\frac{p}{2} K_{comp} \left|I_{comp}\right|^{p-1} \left(\underline{\underline{C}}^{-1} - \frac{1}{I_4}\underline{\underline{M}}\right)$$

$$\underline{\underline{S}}_{dist} = 2K_{dist} I_{dist} \frac{2I_4 \underline{\underline{I}} - (I_1 I_4 - I_5)\underline{\underline{C}}^{-1} + \left(I_1 + \dfrac{I_5}{I_4}\right)\underline{\underline{M}} - 2\left(\underline{\underline{C}} \cdot \underline{\underline{M}} + \underline{\underline{M}} \cdot \underline{\underline{C}}\right)}{4\sqrt{(I_1 I_4 - I_5)^2 - 4I_3 I_4}}$$

$$w_{comp}\left(I_{comp}\right) = \begin{cases} K_{comp}\left|I_{comp}\right|^p & \text{si } I_{comp} \le 0 \\ 0 & \text{si } I_{comp} > 0 \end{cases}$$

Contrainte de Gauss	Raideur du matériau
$\underline{\underline{\sigma}} = \frac{1}{J} \cdot \underline{\underline{F}} \cdot \underline{\underline{S}} \cdot \underline{\underline{F}}^T = \frac{2}{J} \cdot \underline{\underline{F}} \cdot \frac{\partial W}{\partial \underline{\underline{C}}} \cdot \underline{\underline{F}}^T =$	$\underline{\underline{C}} = 2\frac{\partial \underline{\underline{S}}}{\partial \underline{\underline{C}}}$

The volumetric constraint is not explained in the thesis of A. CHARMETANT. The routine he describes is used for the ABAQUS calculation software which works differently compared to ANSYS.

ANSYS recommends describing in code the volumetric behavior of a hyperelastic material because the volume will vary according to the loading directions even if the material is incompressible. This volumetric part is well defined in Sergey Sidorov's thesis, entitled "FINITE ELEMENT MODELING OF HUMAN ARTERY TISSUE WITH A NONLINEAR MULTI-MECHANISM INELASTIC MATERIAL", and dated 2003.

In his Thesis, S. SIDOROV uses ANSYS USERMAT to code another law of hyperelastic material and he specifies that the volumetric stiffness is universal for all hyperelastic materials and equal to: K = 2/d where d is the compressibility coefficient of the material.

If d=0, the material is incompressible and the stiffness is infinite. In our study, we consider a material with d=0.08 MPa-1. As soon as the deviatoric and volumetric stresses are defined, they are summed then entered in an order table (6,1) symbolizing the stress noted on the deformed material.

The routines were programmed in FORTRAN in ANSYS software and tested on a 3D cubic element representing a fiberglass whose properties are available in the ANSYS library
The reading of the output file ".out" shows that the calculation converges well. The displacements and deformation of the element correlates with the fiberglass elongation test curve, stated in the thesis of A. CHARMETANT (Figure 3-3, page 78).

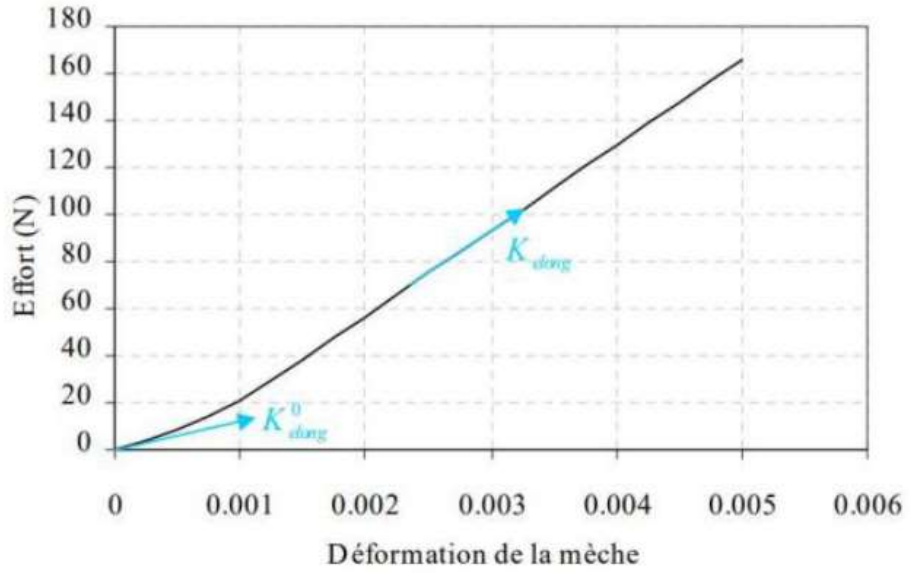

The hyperelastic constitutive law (VUMAT Hyper) was established through a USERRMAT routine in ANSYS for a transverse isotropic hyperelastic material.

The code is mathematically complete but has some weaknesses. The other tests proposed by A. CHARMETANT (compaction, distortion and shearing) were also tested with routine USERMAT. But we note a blocking in the variation of the volume according to the direction X which is weak, even null for these last 3 tests; whereas it is done very well according to the plane transverse to the fiber in Y and Z. This can be characteristic of the stiffness of the material, a concern in the code or an erroneous definition of the limiting conditions of the element. We were unable to resolve this hard point, for lack of time. However, routine USERMAT is still perfectible and it is exploitable for a calculation finite element.

Modeling reinforcements

The hypoelastic model of the grid developed for HOWA-TRAMICO was carried out under ABAQUS with the VUMAT Hypo law.

The simplified reinforcement geometry was measured on the reinforcements.

The objective of these measurements is to be able to provide a Representative Elementary Volume (REV) in order to be able to reconstitute the entire reinforcement as being made up of VER and to make the calculations only on small elements accessible by the computing power at our disposal.

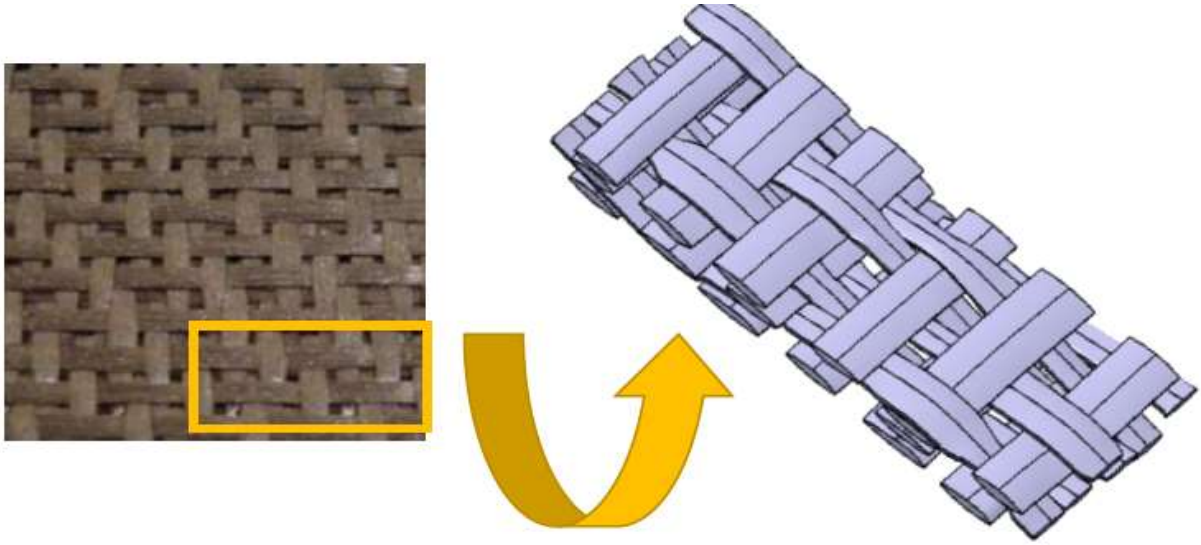

and leads to the following values:

Géométrie du VER

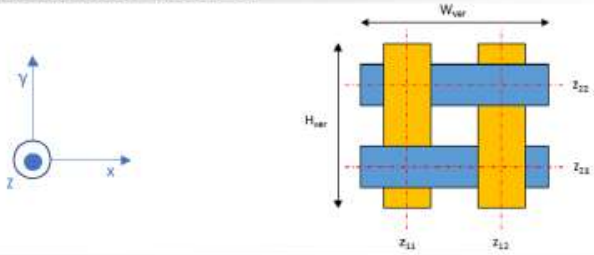

Paramètre	Valeur
W_{VER}	28 mm
H_{VER}	28 mm
z_{11}	7 mm
z_{12}	21 mm
z_{21}	z_{11}
z_{22}	z_{12}

Trajectoires

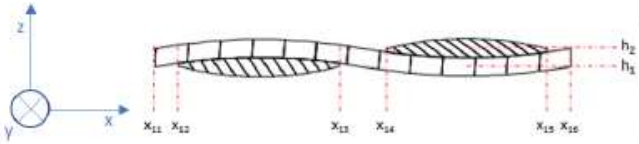

	Param.	Valeurs
Roving 11	x_{11} à x_{16}	0; 3,5; 10,5; 17,5; 24,5; 28
Roving 12	x_{21} à x_{26}	0; 3,5; 10,5; 17,5; 24,5; 28
Roving 21	y_{11} à y_{16}	= x_{11} à x_{16}
Roving 22	y_{21} à y_{26}	= x_{21} à x_{26}
Embuvage	h_1	0
	h_2	0,22

Sections

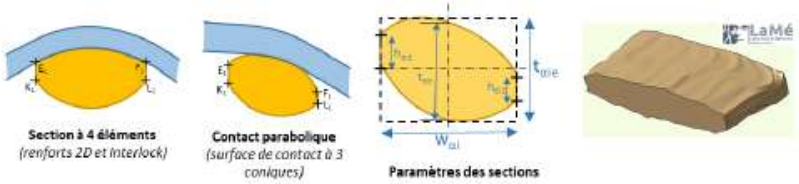

Paramètre	Valeur
f_d	0,08 mm
f_β	= f_d
W_R	7 mm
H_R	0,11 mm

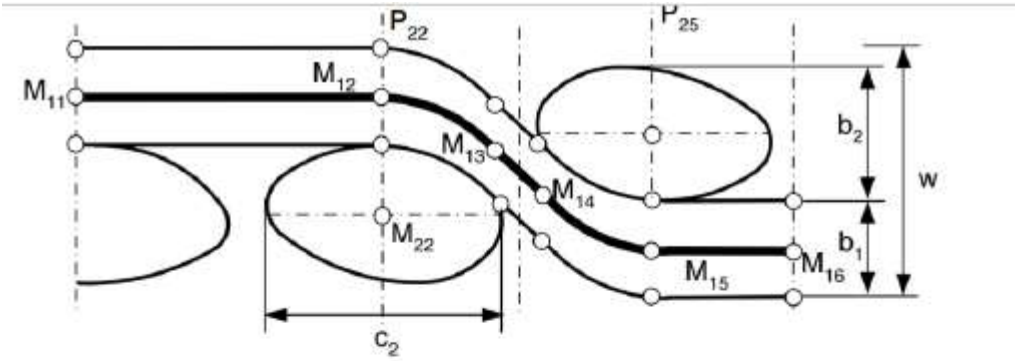

Equation de la trajectoire :

$$(z - z_{S\alpha ik}) = p_{\alpha ik}(x - x_{S\alpha ik})^2,\ 1 \le k \le n_{c\alpha i}$$

Conditions de tangence :

$$2p_{\alpha ik}\left(x_{\alpha ij} - x_{s\alpha ik}\right) = \frac{z_{\alpha ij-1} - z_{\alpha ij}}{x_{\alpha ij-1} - x_{\alpha ij}},\ 1 \le k \le n_{c\alpha i},\ j = 2*k$$

$$2p_{\alpha ik}\left(x_{\alpha ij+1} - x_{s\alpha ik}\right) = \frac{z_{\alpha ij+2} - z_{\alpha ij+1}}{x_{\alpha ij+2} - x_{\alpha ij+1}},\ 1 \le k \le n_{c\alpha i},\ j = 2*k$$

Conditions de périodicité :

$$z_{\alpha i1} = z_{\alpha ij_{max}},\ j_{max} = 2n_{c\alpha i} + 2$$

$$\frac{z_{\alpha i1} - z_{\alpha i2}}{x_{\alpha i1} - x_{\alpha i2}} = \frac{z_{\alpha ij_{max}-1} - z_{\alpha ij_{max}}}{x_{\alpha ij_{max}-1} - x_{\alpha ij_{max}}},\ j_{max} = 2n_{c\alpha i} + 2$$

Behavioral law of 2D reinforcements (base UD) is carried out from characterization tests of the rovings and the determination of the law of behavior of the homogeneous material equivalent to the fibrous material, from the analysis of the behavior of the rovings and the interactions between them (inherited from the behavior of the assembly of bundles of unit fibers that compose it and their interactions).

Dépendance V_f	fil	S_0	K_{elong}	K_{cis}	K_{comp}	P_{comp}	K_{dist}	P_{dist}
		mm²	N	MPa	kPa	-	kPa	-
avec	trame	0.17	16800	5	80	2.05	60	2.03
	chaîne	0.76	16800	5	300	2	250	2
sans	trame	0.17	16800	5	45	4.2	15	5
	chaîne	0.76	16800	5	45	4.2	15	5

The stack considered is 4 plies of linen UD (with weft yarn):

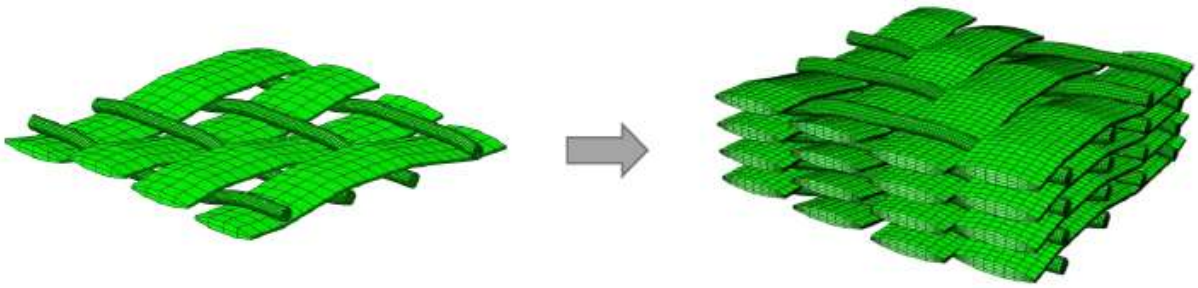

The calculation converges towards a compacted structure making it possible to establish the parameters of porosity, free volume and volume of fiber on the compressed structures during implementation.

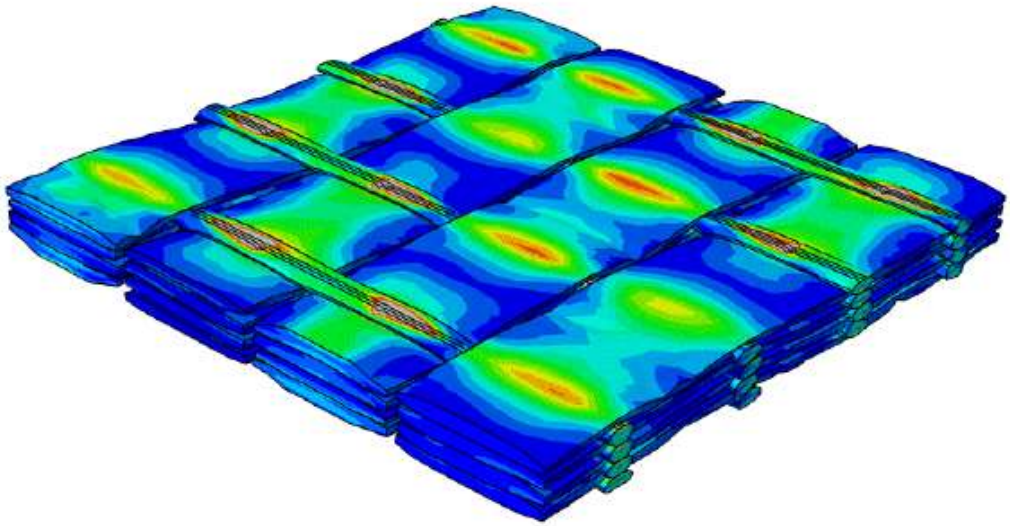

Conclusions and perspectives

This fundamental work has highlighted the complexity of taking into account the behavior law of oriented fibrous network during the stresses exerted on the dry reinforcements during their implementation in the manufacturing processes of composite materials.
We have two VUMATs to model the modifications of the fibrous reinforcements and the first results show a good correlation with the tests (Hypo).

Work remains to be done to finalize the VERs of the NCF reinforcements developed in the FLOWER project and to correlate the results of the models with the impregnation performance measured on the NCF materials by the University of Cambridge.